A set of calculation tools supporting the design, modelling and application of plywood-based seismic retrofitting interventions on timber floors in existing buildings

Mirra, Michele

DOI
10.1016/j.istruc.2024.106378

Publication date
2024

Document Version
Final published version

Published in
Structures

Citation (APA)
Mirra, M. (2024). A set of calculation tools supporting the design, modelling and application of plywood-based seismic retrofitting interventions on timber floors in existing buildings. *Structures*, *63*, Article 106378. https://doi.org/10.1016/j.istruc.2024.106378

Structures 63 (2024) 106378

Contents lists available at ScienceDirect

Structures

journal homepage: www.elsevier.com/locate/structures

A set of calculation tools supporting the design, modelling and application of plywood-based seismic retrofitting interventions on timber floors in existing buildings

Michele Mirra

Department of Engineering Structures, Section of Biobased Structures and Materials, Delft University of Technology, Stevinweg 1, 2628 CN Delft, The Netherlands

ARTICLE INFO

Keywords:
Timber Floors
Plywood
Seismic retrofitting
Architectural Conservation
Design Tools
Numerical Analyses

ABSTRACT

The application of timber-based strengthening solutions to existing wooden and masonry structures, combines several benefits, such as reversibility, compatibility, lightness, sustainability, affordability, and effectiveness. With reference to existing timber floors, an efficient method to enhance their seismic response is the fastening of an overlay of plywood panels to the existing sheathing, an intervention that greatly improves in-plane strength, stiffness, and energy dissipation. In order to promote the use of this retrofitting solution in practice, this work presents a set of calculation tools supporting the design and advanced numerical modelling of timber diaphragms strengthened with plywood panels. The suite of tools allows to first estimate the full nonlinear, cyclic in-plane response of the strengthened diaphragms starting from the geometrical and material properties of the existing sheathing and the plywood overlay, as well as the mechanical characteristics of the fasteners. As second step, such estimated in-plane response can be transformed into a constitutive law for performing nonlinear numerical simulations, by means of a user-supplied subroutine developed for finite element software DIANA FEA. The presented calculation examples and the performed validation against reference studies from literature, show that the developed tools can provide an accurate estimate of the in-plane response of the diaphragms, and enable an efficient numerical simulation of their seismic behaviour. The implemented tools can be used to both obtain preliminary indication for plywood-based seismic retrofitting design, and to calibrate the interventions on existing diaphragms based on the specific characteristics and needs of a building, relying on the adaptability and versatility of this strengthening method.

1. Introduction

1.1. Background

Unreinforced masonry constructions featuring timber floors as horizontal structural elements, constitute a large part of the building stock in numerous seismic-prone architectural contexts. The observed damage to these buildings already for moderate earthquakes, has highlighted their vulnerability to seismic actions, mainly due to poor-quality masonry, excessive in-plane flexibility of timber floors, and absence of effective connections among structural elements. In this framework, several research studies on seismic characterisation and retrofitting of timber diaphragms [1–15] and timber-masonry connections [16–23] have been conducted in the recent years, progressively focusing on more reversible techniques [24]. With specific regard to the floors, the main proposed and tested retrofitting methods consisted of the traditional cast of a concrete slab on the existing sheathing, a widely adopted retrofitting in the last decades [1,5]; the superposition of a second layer of planks arranged at 45° [1–3] or 90° [5,6] with respect to the existing sheathing; the bracing of the floors with steel plates [1,3] or fibre reinforced polymer (FRP) laminae [1,5]; the overlay of cross-laminated timber (CLT) [6–9], oriented strand board (OSB) [7,10], or plywood panels [11–15].

Among these techniques, reversible solutions are usually preferred because of their lower impact on existing buildings, especially when they are monumental or protected [24–28]. In particular, the overlay of plywood panels on the existing sheathing has proved to be a valid and versatile strengthening method, as demonstrated by several investigations and practical applications in different contexts, e.g. in the United States [11,29,30], New Zealand [12–14,31], the Netherlands [15,32–35], and Italy [26,36–39].

Besides improving in-plane strength and stiffness of the existing

E-mail address: M.Mirra@tudelft.nl.

https://doi.org/10.1016/j.istruc.2024.106378
Received 8 February 2024; Received in revised form 27 March 2024; Accepted 5 April 2024
Available online 10 April 2024

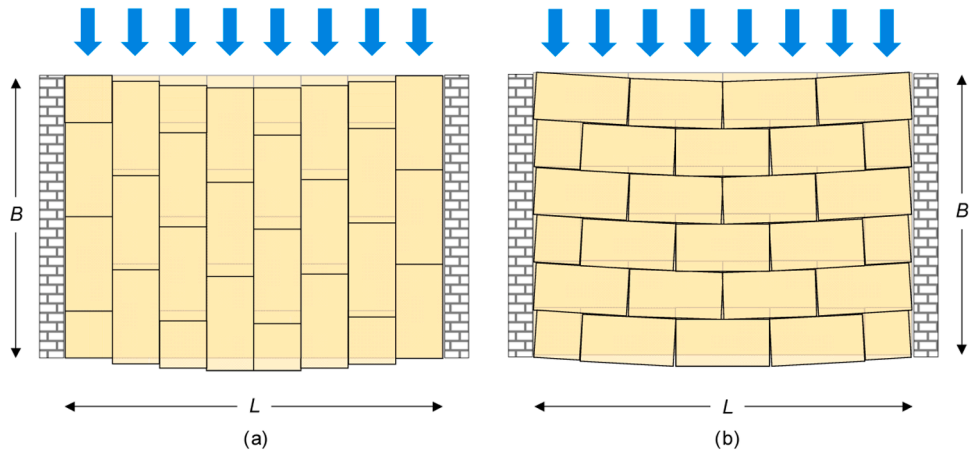

Fig. 1. In-plane deflection of timber diaphragms retrofitted with plywood panels: (a) the response is dominated by panels' sliding when their long side is parallel to the load; (b) the response is dominated by panels' rotation and interlocking when their long side is perpendicular to the load.

floors, the plywood-based retrofitting also provides additional capacity in terms of ductility and energy dissipation [13,31,34,35,37], mainly because of the yielding of the numerous fasteners, provided that effective connections are realized between timber and masonry structural elements [16–19,22,28,31]. Along with such advantages, this strengthening method also features practical benefits from the professional engineering perspective, such as affordability, ease and rapidity of application, compatibility with the existing structure, reversibility, sustainability, and effectiveness [36,37].

1.2. Overview of the set of calculation tools

In light of the aforementioned investigations and findings, to promote timber-based seismic retrofitting techniques and facilitate the adoption and application of this strengthening method among professional engineers, this work presents a set of tools supporting the design and modelling of plywood-retrofitted diaphragms.

First, nomograms were derived, allowing practitioners to perform a preliminary, expeditious design of the retrofitting interventions. The nomograms are based on a refinement and extension of previously formulated analytical models [32], which also form the background of a more comprehensive calculation tool (*ApPlyWood*) that was implemented in *Python* programming language [40]. This software provides an estimate of the full, cyclic in-plane response of the strengthened diaphragms, starting from the geometrical and material properties of existing floor, plywood overlay, and fasteners. Finally, a user-supplied subroutine (*SimPlyWood*) for finite element software DIANA FEA [41] was developed, enabling the numerical simulation of the in-plane response of the retrofitted floors based on a macro-elements approach. *ApPlyWood* and *SimPlyWood* are available as a single collection of tools at the following link: https://doi.org/10.4121/8a09d423–2acc-4c7f-86af-90b5adca4660.

Before describing in detail the developed tools and their application, the analytical framework behind them is recalled in Section 2, along with the adopted methodology. Subsequently, Section 3 reports and discusses the use of the nomograms and *ApPlyWood* calculation tool, while Section 4 focuses on the implemented subroutine *SimPlyWood*. For both design and modelling tools, calculation examples are provided. Finally, in Section 5 the concluding remarks of this work are reported.

2. Methodology at the basis of the developed tools

2.1. Brief recall of the analytical framework

The adopted analytical formulation at the basis of the developed tools consists of a refinement of a previously derived model to predict the in-plane response of diaphragms retrofitted with plywood panels fastened along their perimeter to the existing sheathing, starting from the load-slip response of a single fastener [32,33]. This load-slip curve is determined as a combination of a linear and a parabolic branch, representing the initial stiffness and the global behaviour, respectively:

$$F_f = (F_{0,f} + a{\cdot}u_f + b{\cdot}u_f^2)\left[1 - \exp\left(-\frac{K_{0,f}}{F_{0,f}}u_f\right)\right] \geq 0;\ \text{with } a > 0,\ b < 0 \tag{1}$$

In Equation 1, F_f and u_f are the force and displacement of the fastener, respectively; $F_{0,f}$, a and b are the coefficients of the parabola representing the global behaviour, while $K_{0,f}$ is the slope of the line representing the initial stiffness [32]. The failure criterion for the curve is defined in agreement with the provisions of ISO 16670:2003 [43], thus when the transferred load drops below 80 % of the peak strength during the softening phase.

All parameters of Eq. 1 can be derived from tests on single joints [32], but can also be analytically estimated, should such tests not be available [32,33]. The following expression for the initial stiffness $K_{0,f}$ (N/mm), determined directly from the nominal diameter d of the fastener (mm), was found to provide very accurate values [44]: $K_{0,f} = 50d^{1.7}$.

The yielding load of the fastener $F_{0,f}$ can be predicted starting from the knowledge of the maximum force $F_{max,f}$ determined according to EN 1995:2004 [45] and Johansen's theory for timber-to-timber joints [46], assuming a fastener sufficiently slender to develop two plastic hinges. Then, $F_{0,f}$ can be estimated as $F_{max,f}/8$ for screws, and $0.4F_{max,f}$ for nails, in agreement with prior experimental tests [7,13,32].

Finally, the two parameters a and b, describing the parabolic branch, are expressed as:

$$a = 2\frac{F_{\max,f} - F_{0,f}}{u_{\max,f}} \tag{2}$$

$$b = -\frac{F_{\max,f} - F_{0,f}}{u_{\max,f}^2} \tag{3}$$

In Eqs. 2 and 3, $u_{max,f}$ is the slip of the fastener at $F_{max,f}$; this can be estimated as $u_{max,f} = (b_1{+}b_2)\tan\alpha$ [32], with $(b_1{+}b_2)$ distance between the two plastic hinges of the fastener in the two members of the joint according to Johansen's theory [46], and α angle at which the yield moment of the fastener is evaluated, according to EN 409:2009 [47]. The angle α should be at least 45° for nails, and $110/d_1$ degrees for screws, with d_1 shank diameter [32,47].

Starting from the load-slip curve of the single screw, the in-plane response of a whole retrofitted floor is derived considering equilibrium relations [32], treating the diaphragm as a shear wall, and

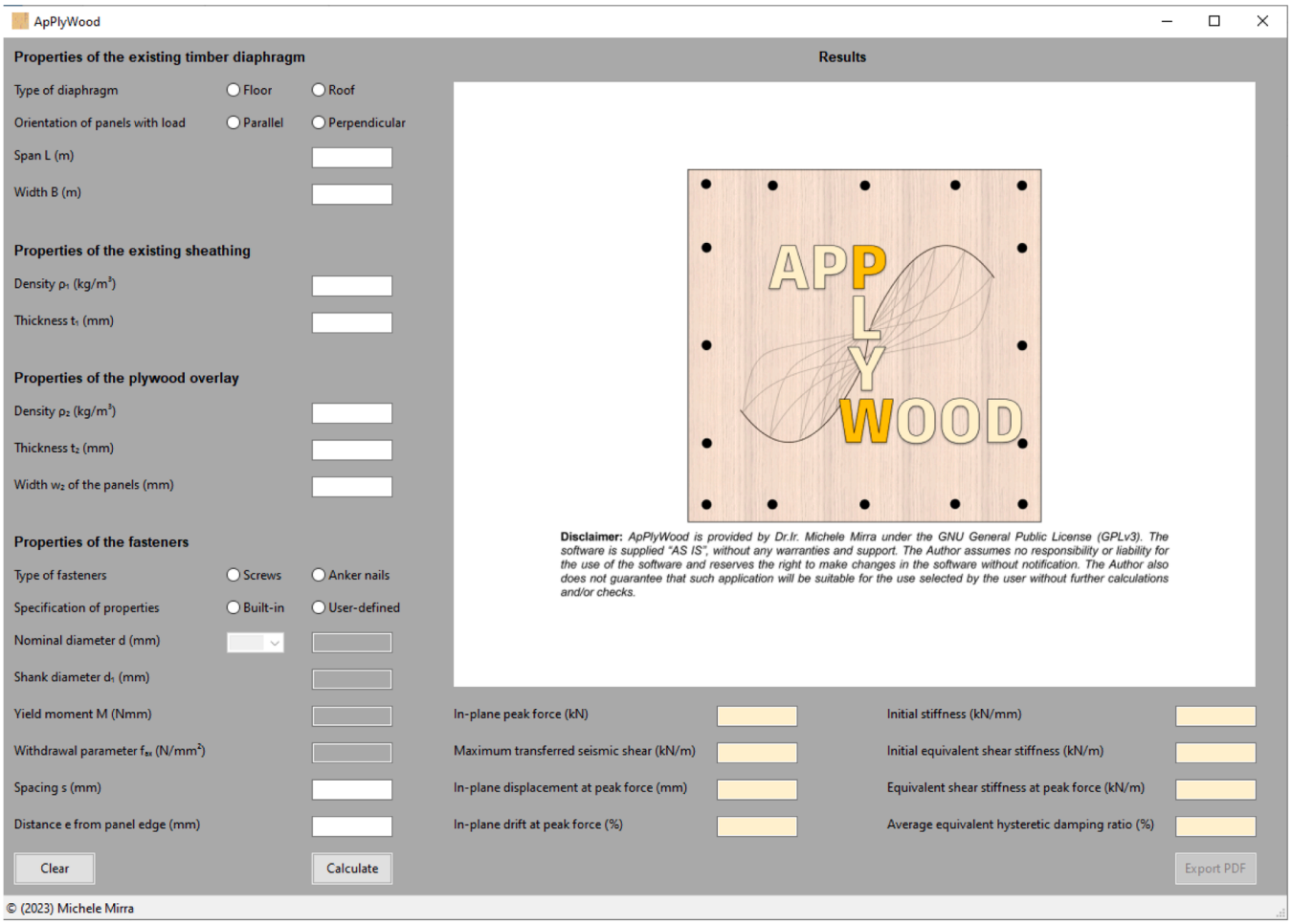

Fig. 2. Graphical user interface of *ApPlyWood* calculation tool.

accounting for its different behaviour depending on the panels' layout (Fig. 1). When the panels are oriented with their long side parallel to the in-plane load (Fig. 1a), the response is dominated by sliding among the panels themselves, with no interlocking [7,13,14,31]; in this case, the in-plane deflection of the diaphragm depends on the number of fasteners' shear planes parallel to the loading direction, since each line contributes with its own slip to the total displacement. When the panels are oriented with their long side perpendicular to the in-plane load (Fig. 1b), the response is influenced by the rotation of the panels, and an improved performance because of interlocking and frictional effects is obtained [14,15,31]. Such improved behaviour under the loading configuration of Fig. 1b was accounted for as an increase in strength ΔF (in kN) depending on the in-plane drift γ [32], based on the outcomes of previous sensitivity analyses [14]: $\Delta F = 1.05 + 10\,\gamma$.

The here recalled analytical framework has been formulated in previous research studies [32,33], to which the reader is referred for further details, and serves as a basis for the implementation of the calculation tools and the subroutine, presented in the following.

2.2. Derivation of nomograms and development of ApPlyWood calculation tool

The nomograms, presented in Section 3, were constructed on the basis of the aforementioned analytical formulation. These tools can be used for an expeditious, graphical estimate of the strength and stiffness of the retrofitted diaphragms. The nomograms were derived under the following assumptions:

- A retrofitted diaphragm of width B and span L (Fig. 1), assumed as a simply supported beam under distributed in-plane load, is considered; the panels, placed in a staggered layout, are fastened along their perimeter to the underlying planks, which are able to transfer shear forces;
- Two panels' dimensions are examined: 600×1200 mm and the usual 1200×2400 mm; for intermediate values, linear interpolation can be used;
- Loading parallel or perpendicular to the long side of the panels is considered;
- A typical configuration is assumed, with sheathing thickness $t_1 = 18$ mm and density $\rho_1 = 420$ kg/m^3; plywood thickness $t_2 = 18$ mm and density $\rho_2 = 500$ kg/m^3;
- The obtained strength values refer to widely used fasteners (screws, in this case), having a length at least equal to the sum of the thickness of sheathing and plywood overlay, and for which detailed mechanical properties are available [48]; the screws are sufficiently slender with respect to the thickness of connected members, so as to guarantee the formation of two plastic hinges.

Such constructed nomograms allow to graphically determine, as a function of different diameters and spacing of the screws, the seismic shear $v = F_{max,floor}/(2B)$ that the diaphragm is able to transfer (left axis, in kN/m) based on its strength $F_{max,floor}$, along with the corresponding equivalent shear stiffness G_d at peak load (right axis, in kN/m). In order to account for configurations deviating from that assumed, specific adjustment factors were also derived, in such a way that the corresponding values of shear strength v' and equivalent shear stiffness G'_d

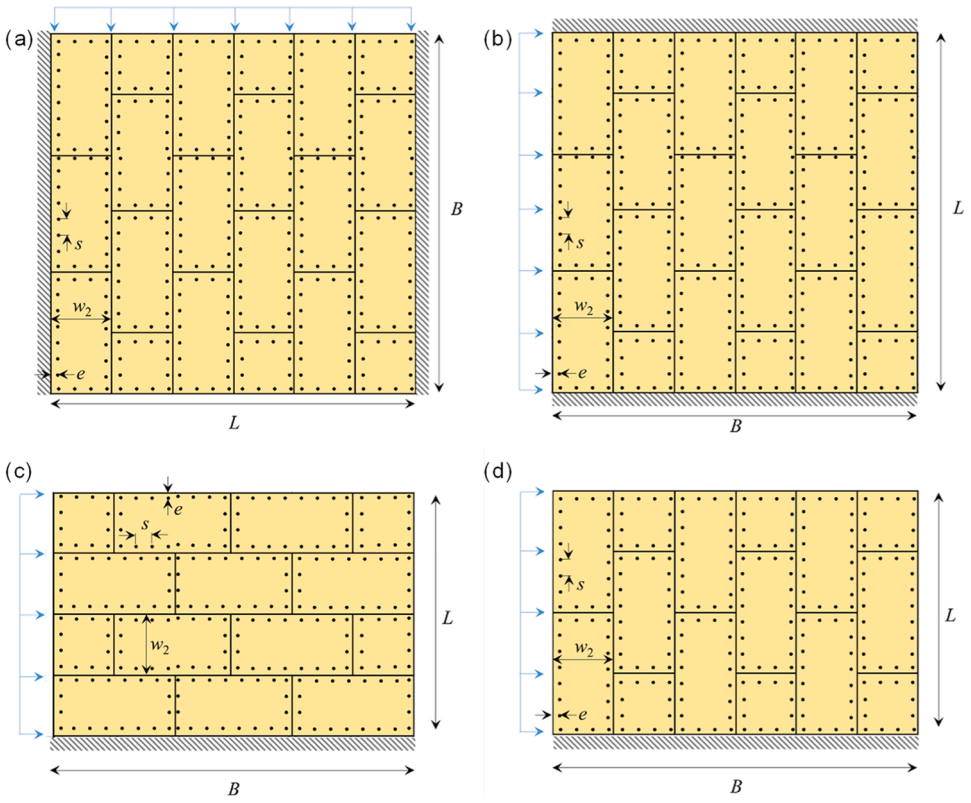

Fig. 3. Schematic images of the retrofitted diaphragms appearing in the calculation tool, aiding the user during the parameters' selection: floor having panels oriented parallel (a) and perpendicular (b) to the seismic action; in-plane loaded roof pitch having panels oriented parallel (c) and perpendicular (d) to the seismic action.

could still be estimated from those reported in the nomograms:

$$v' = k_t \cdot k_{\rho,v} \cdot v \tag{4}$$

$$G_d' = k_t \cdot k_{\rho,v} \cdot k_{\rho,G} \cdot G_d \tag{5}$$

In equations 4 and 5, k_t accounts for variations in thickness, $k_{\rho,v}$ for variations in density in terms of strength, and $k_{\rho,G}$ for variations in density in terms of equivalent shear stiffness; nomograms for these coefficients were also derived (Section 3). In this way, by knowing the expected seismic shear to be transferred, and/or the maximum allowable in-plane drift for the diaphragm, it is possible to proceed with a simplified, expeditious design of the retrofitting, aided by the derived graphs.

Next to the nomograms, in order to display the full, cyclic nonlinear in-plane response of the retrofitted diaphragms, a calculation tool (*ApPlyWood*, Fig. 2) was also implemented in *Python* programming language [40]; the user interface was realised with *wxPython* toolkit [42]. The calculations performed within the software are entirely based on the presented analytical formulation [32]: the in-plane response is determined constructing the diaphragm's backbone curve and deriving the internal pinching cycles on the basis of a geometrical procedure developed in previous studies [32,33] and described in detail in Section 2.3, related to the user-supplied subroutine implementation. The reference displacements at which the pinching cycles are calculated correspond to the steps prescribed by ISO 16670:2003 [43], assuming as ultimate displacement the value $d_{max,floor}$ at which the strength $F_{max,floor}$ is reached.

The user needs to first specify the type of diaphragm (floor or roof; the latter case refers to in-plane loaded pitches, where the span to be specified is their inclined length), the panel orientation with respect to the load (parallel or perpendicular, influencing the in-plane response as previously shown in Section 2.1 and Fig. 1), and the main dimensions L and B. During the selection, a schematic picture of the diaphragm appears (Fig. 3), to help the user specify all required parameters. Next, the material and geometrical properties of both existing sheathing and plywood panels have to be inserted, followed by the characteristics of the fasteners. In this case, the user can specify the utilization of screws or Anker nails, and can refer to built-in properties (based on available technical data [48]), or user-defined ones, to be manually input. Finally, the spacing and distance from panel edge of the selected fasteners have to be inserted.

By pressing the *Calculate* button, the software plots the estimated nonlinear, cyclic in-plane response of the designed diaphragm following ISO 16670:2003 [43], along with a miniature of the selected static scheme from Fig. 3. Should an input parameter be missing for any reason, the bottom status bar will indicate it. Otherwise, the bottom status bar displays the statement *In-plane response of the diaphragm successfully determined*, and the button *Export PDF* is enabled. This allows the user to save a one-page PDF report of the graph with the main output values. Finally, the button *Clear* allows to clear all fields and restart with another calculation.

Along with the graph of the in-plane response of the retrofitted diaphragm, the tool provides as output the global peak force $F_{max,floor}$, its associated transferred seismic shear $v = F_{max,floor}/(2B)$, the corresponding displacement $d_{max,floor}$ along with the drift γ, the initial stiffness $K_{0,floor}$ and corresponding initial equivalent shear stiffness $G_{d,0}$, the equivalent shear stiffness at peak force G_d, and the average equivalent hysteretic damping ratio ξ_{av} (calculated with the energy loss per cycle method [49]) over all pinching cycles.

ApPlyWood is downloadable as *Python* script (optimized for Windows and Mac OS) or standalone executable (for Windows only) at https://doi.org/10.4121/10125465–64bf-46f3-a2e3-d7ce7ae78cf8, and is provided under the GNU General Public License (GPLv3). In Section 3, two calculation examples and a comparison with experimental

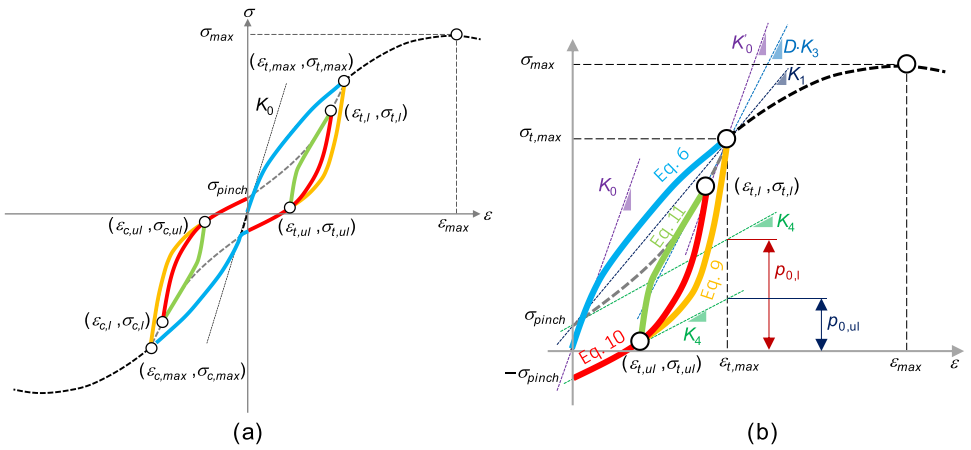

Fig. 4. (a) graphical representation of the constitutive law implemented in the subroutine and representing the in-plane response of the retrofitted diaphragms: the input and state variables are also indicated; (b) detailed overview of the loading, unloading and reloading branches along with the main parameters and associated equations in the article text.

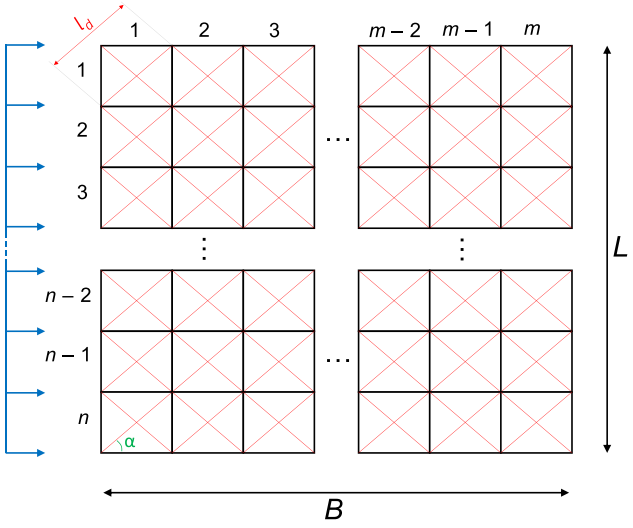

Fig. 5. Schematic representation of a diaphragm simulated with macro-elements.

outcomes from literature, are presented.

2.3. Subroutine implementation (SimPlyWood package)

After designing and estimating the in-plane response of plywood-retrofitted diaphragms with *ApPlyWood* calculation tool, an additional package (*SimPlyWood*) was developed, containing a user-supplied subroutine enabling their numerical simulation, and a spreadsheet to transform the design values from *ApPlyWood* into the input values for the subroutine, which was implemented to be compatible with the finite element software DIANA FEA [41]. This software is widely used to assess the structural and seismic response of masonry structures, and allows utilizers to provide user-supplied materials. In light of the frequent presence of wooden floors and roofs in masonry buildings, an additional tool for the advanced modelling of the seismic response of retrofitted timber diaphragms could be beneficial for a more complete structural assessment within the same software.

The subroutine was developed considering a macro-element approach as numerical simulation strategy for retrofitted diaphragms, also adopted in previous studies [27,32–35]. These macro-elements consisted of quadrilaterals of rigid truss elements, surrounding two diagonal truss elements, in which the nonlinear in-plane behaviour of the floor was implemented adopting the proposed analytical model (see Figs. 4 and 5). Such modelling strategy proved to be accurate and efficient, enabling to simulate the in-plane response of the diaphragms by means of uniaxial constitutive laws. The macro-elements can also be combined with linear elastic orthotropic plate elements for simulating the out-of-plane (static) response of the floors [33–35]. It should be noticed that, unlike other implementations, e.g. *ZeroLength* elements in *OpenSees* software [50], in DIANA FEA the two in-plane loading directions cannot be fully uncoupled, accounting for the in-plane orthotropy of the retrofitted diaphragms as represented in *ApPlyWood* tool. However, usually at global building level seismic strengthening interventions on the diaphragms are designed to prevent the excessive in-plane deflection of their longer sides or in correspondence to locations where masonry is most vulnerable to out-of-plane loads. Based on this, the nonlinear response along the governing loading direction can thus be assigned to the macro-elements, also in light of frequent measures that are applied in combination with the in-plane strengthening of the floors, and that can in the end (strongly) reduce their orthotropic behaviour, such as panels' blocking [11], use of timber blocks or steel elements/chords for connecting the diaphragms to the masonry [13,15,22], or a more interlocked panels' layout [14,31], which can also be well represented through the developed tools (Section 3.2.3).

In order for the user-supplied subroutine to be compatible with the DIANA FEA environment, the constitutive laws for the diagonal trusses of the macro-elements were implemented adopting FORTRAN 90 programming language [51]. Three types of input variables are required by a DIANA FEA subroutine:

- user-specified initialization variables, not changing within the calculations performed in the subroutine;
- initial state variables, varying during the calculations performed in the subroutine, for instance to determine loading and unloading points;
- initial indicator variables (not applicable for this case and set to 0).

As output, DIANA FEA requires user-supplied subroutines to provide the stress-strain relation of the material, to be adopted at every calculation step.

Four relevant initialization variables are needed: the strain ε_{max} at peak stress σ_{max}, the peak stress σ_{max} itself, the initial elastic modulus K_0 (Fig. 4), and a *FASTENER* variable identifying the fastener type (0 = nails; 1 = screws). These variables are known, once the diaphragm's retrofitting has been designed according to the expected seismic loads, with the support of *ApPlyWood* calculation tool. Besides, ten initial state variables were adopted, necessary for describing all loading and

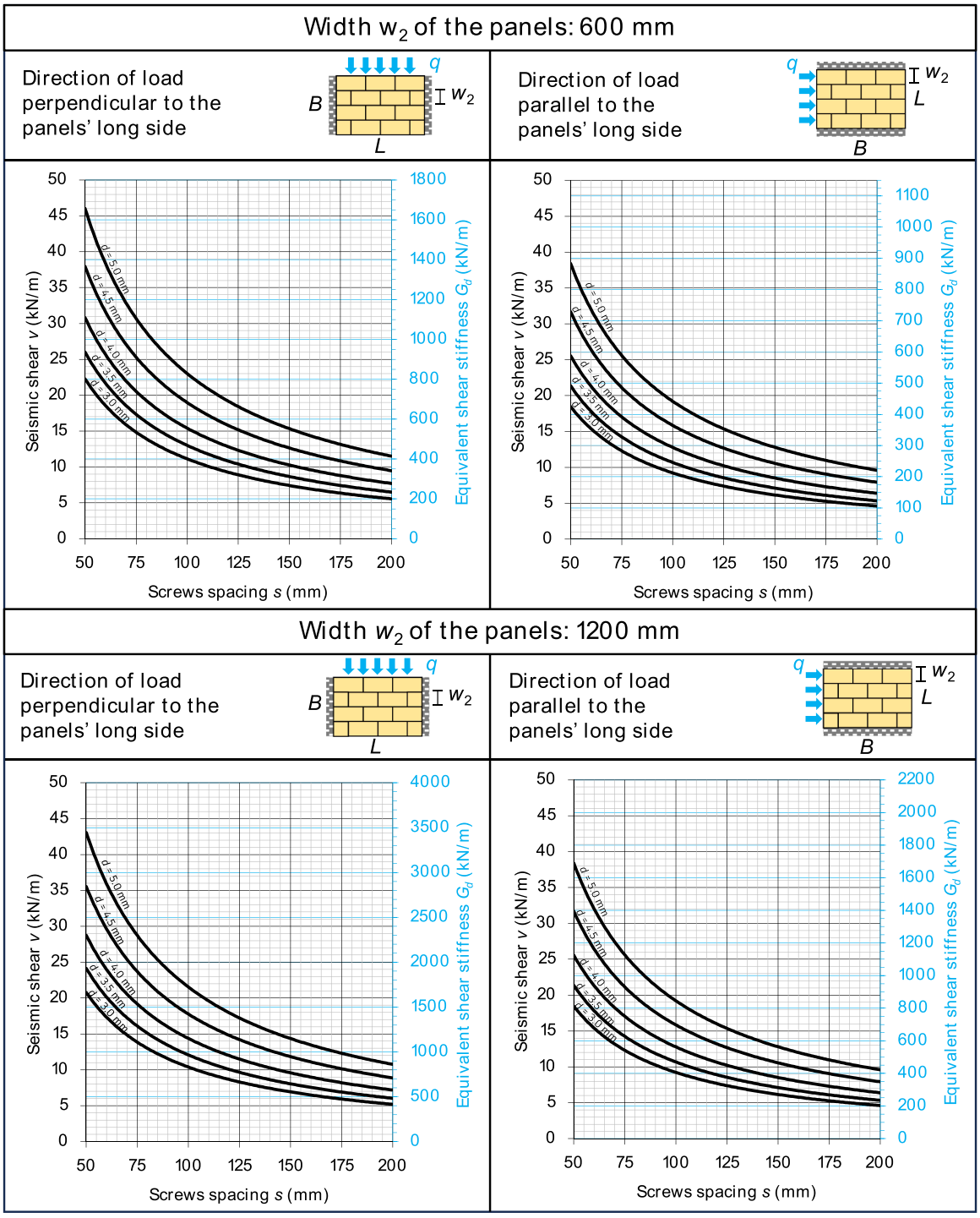

Fig. 6. Nomograms for graphically retrieving in-plane strength and equivalent shear stiffness of the retrofitted diaphragms as a function of screws' diameter and spacing, and panels' width and layout.

unloading branches; their initial value is set to 0. With reference to Fig. 4a, these parameters are:

- the maximum strains ever reached in tension and compression ($\varepsilon_{t,max}$ and $\varepsilon_{c,max}$, respectively);
- the stress-strain coordinates identifying the end of the loading and unloading branches in tension, i.e. points ($\varepsilon_{t,l}$,$\sigma_{t,l}$) and ($\varepsilon_{t,ul}$,$\sigma_{t,ul}$), respectively;
- the stress-strain coordinates identifying the end of the loading and unloading branches in compression, i.e. points ($\varepsilon_{c,l}$,$\sigma_{c,l}$) and ($\varepsilon_{c,ul}$,$\sigma_{c,ul}$), respectively.

These variables enabled the description of the complex unloading and reloading behaviour given by the pinching cycles (Fig. 4a). The constitutive laws implemented in the user-supplied subroutine are now presented in the following for the tensile branch, since the compressive one features antisymmetric relations.

The material follows the tensile loading branch until when $\varepsilon > 0$ and

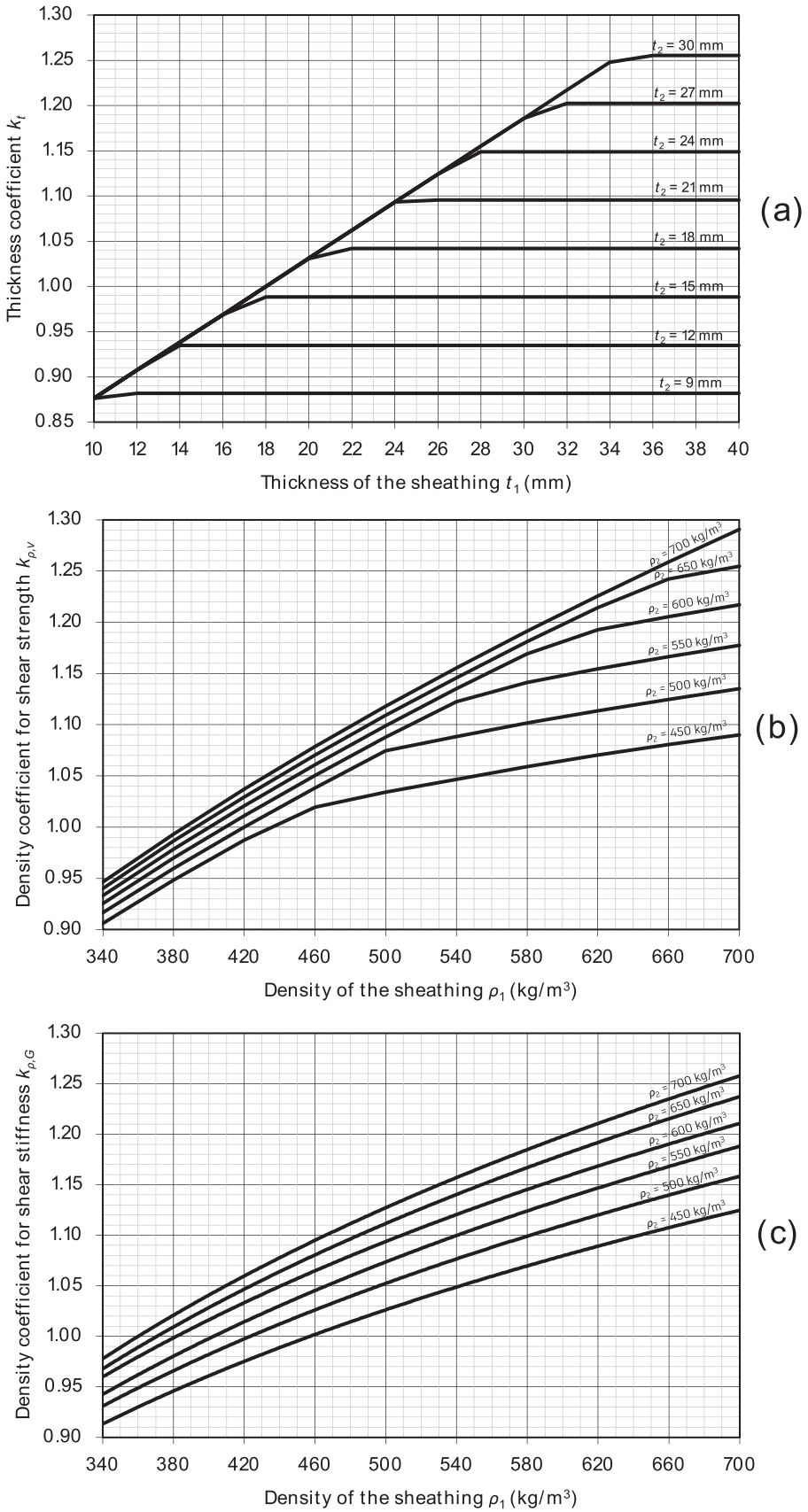

Fig. 7. Nomograms for coefficients k_t (a), $k_{\rho,v}$ (b), and $k_{\rho,G}$ (c) of Eqs. 4 and 5, referred to screws.

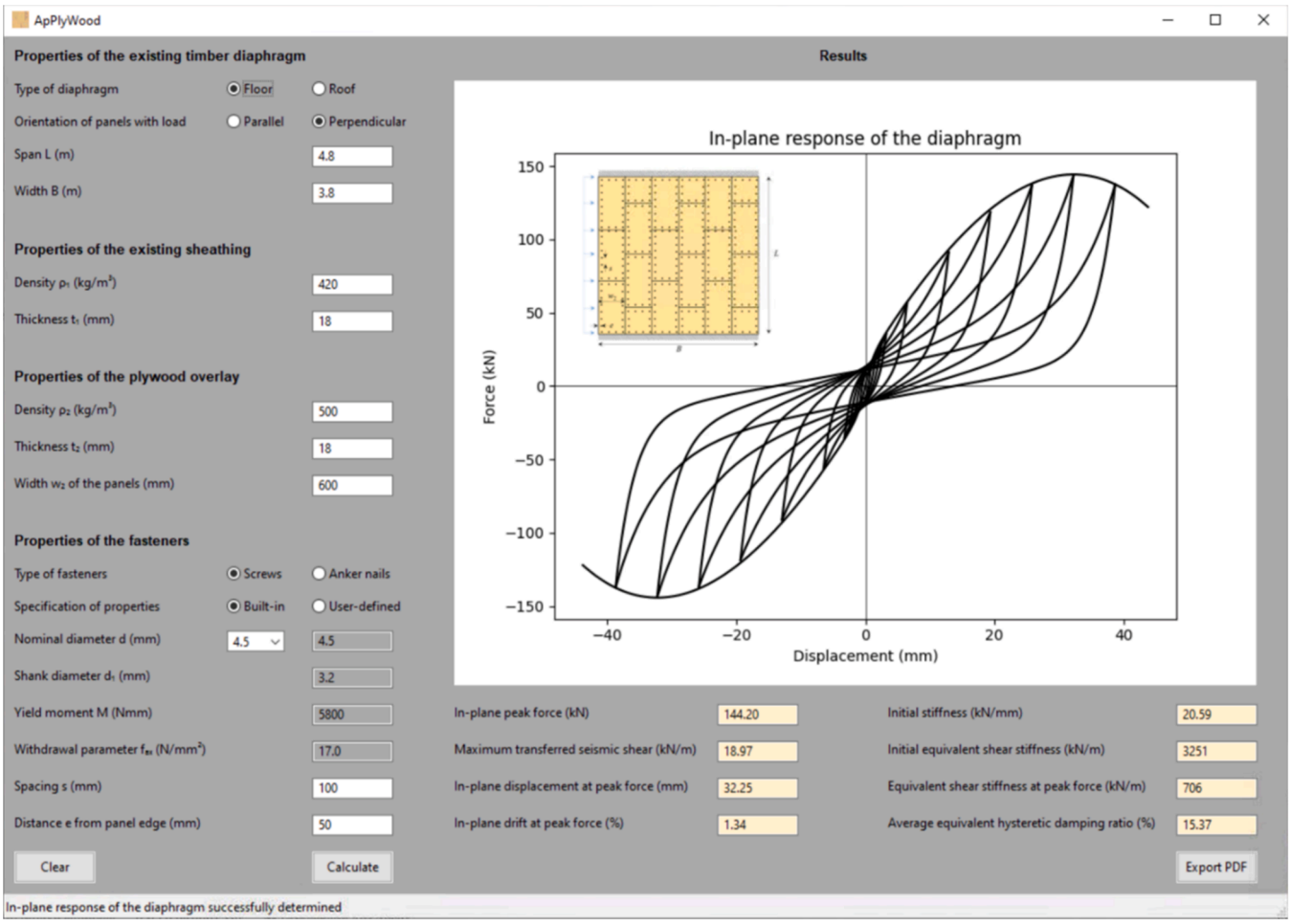

Fig. 8. First calculation example executed with *ApPlyWood*.

contemporarily $\varepsilon > \varepsilon_{t,max}$, with the constitutive law of Eq. 6 (Fig. 4b, blue branch), which corresponds to Eq. 1 written in stress-strain form:

$$\sigma = (\sigma_y + a{\cdot}\varepsilon + b{\cdot}\varepsilon^2)\left[1 - \exp\left(-\frac{K_0}{\sigma_y}\varepsilon\right)\right]. \tag{6}$$

In Eq. 6, $\sigma_y = 0.4\sigma_{max}$ for nails ($FASTENER = 0$) and $\sigma_y = \sigma_{max}/8$ for screws ($FASTENER = 1$), following the analytical formulation of Section 2.1. Before presenting the constitutive laws for the pinching cycles, a number of constructions lines are defined, with reference to Fig. 4b and to the geometrical procedure adopted for deriving such cycles, presented in a previous study [32]. Firstly, the positive intercept of the pinching cycles is set at $\sigma_{pinch} = 0.1\sigma_{max}$. The stiffness K_3 is the bisector [32] of the lines having slopes K_0' $= K_0$, and $K_1 = (\sigma_{t,max} - \sigma_{pinch})/\varepsilon_{t,max}$ (Fig. 4b). The stiffness K_4 is the slope of the line joining σ_{pinch} with the point on the bisector having a strain equal to $\varepsilon_{t,max}/2$: $K_4 = (\sigma_{t,max} - K_3\ \varepsilon_{t,max}/2 - \sigma_{pinch})/(\varepsilon_{t,max}/2)$, in agreement with the previously developed analytical model [32]. Finally, the quantities $p_{0,l}$ and $p_{0,ul}$ are defined, following Eqs. 7 and 8 (Fig. 4b):

$$p_{0,l} = \sigma_{pinch} + K_4\varepsilon_{t,\max} \tag{7}$$

$$p_{0,ul} = -\sigma_{pinch} + K_4\varepsilon_{t,\max} \tag{8}$$

Now, the unloading and reloading phases of the pinching cycles can be derived. After reaching $\varepsilon_{t,max}$, the tensile unloading phase takes place when $\varepsilon > 0$, $\varepsilon < \varepsilon_{t,max}$, and $\varepsilon < \varepsilon_0$, with ε_0 initial strain at the beginning of the current step. The unloading response is formulated in two different cases: when the unloading starts from the loading branch (at $\varepsilon_{t,max}$, yellow branch of Fig. 4b), and when the unloading occurs after a reloading phase (red branch of Fig. 4b). In the first case, $\varepsilon_{t,l} \equiv \varepsilon_{t,max}$, and the constitutive law is formulated as (see Fig. 4b for the meaning of the various parameters):

$$\begin{aligned}\sigma &= f_{t,ul} \\ &= \sigma_{t,\max} - [\sigma_{t,\max} - p_{0,ul} - K_4(\varepsilon - \varepsilon_{t,\max})]\{1 - \exp[2K_0(\varepsilon - \varepsilon_{t,\max})/(\sigma_{t,\max} - p_{0,ul})]\}\end{aligned} \tag{9}$$

In the second case, the following relation applies:

$$\sigma = \sigma_{t,l} - (\sigma_{t,l} - f_{t,ul})\{1 - \exp[2K_0(\varepsilon - \varepsilon_{t,l})/(\sigma_{t,l} - f_{t,ul})]\} \tag{10}$$

Finally, tensile reloading takes place when $\varepsilon > 0$, $\varepsilon < \varepsilon_{t,max}$, and $\varepsilon > \varepsilon_0$, according to the constitutive law of Eq. 11 (green branch in Fig. 4b):

$$\sigma = \sigma_{t,ul} + (f_{t,l} - \sigma_{t,ul})\{1 - \exp[-2K_0(\varepsilon - \varepsilon_{t,ul})/(f_{t,l} - \sigma_{t,ul})]\} \tag{11}$$

with:

$$f_{t,l} = \sigma_{t,\max} - [\sigma_{t,\max} - p_{0,l} - K_4(\varepsilon - \varepsilon_{t,\max})]\{1 - \exp[D{\cdot}K_3(\varepsilon - \varepsilon_{t,\max})/(\sigma_{t,\max} - p_{0,l})]\} \tag{12}$$

and:

$$D = 1 + (\varepsilon_{t,\max}/\varepsilon_{\max})^3 \tag{13}$$

With reference to Eq. 13, the parameter D is a factor accounting for the progressive degradation occurring in the pinching cycles (Fig. 4b), which dissipate less hysteretic energy when the floor's drift increases [32,33].

The implemented subroutine, part of the *SimPlyWood* package, can

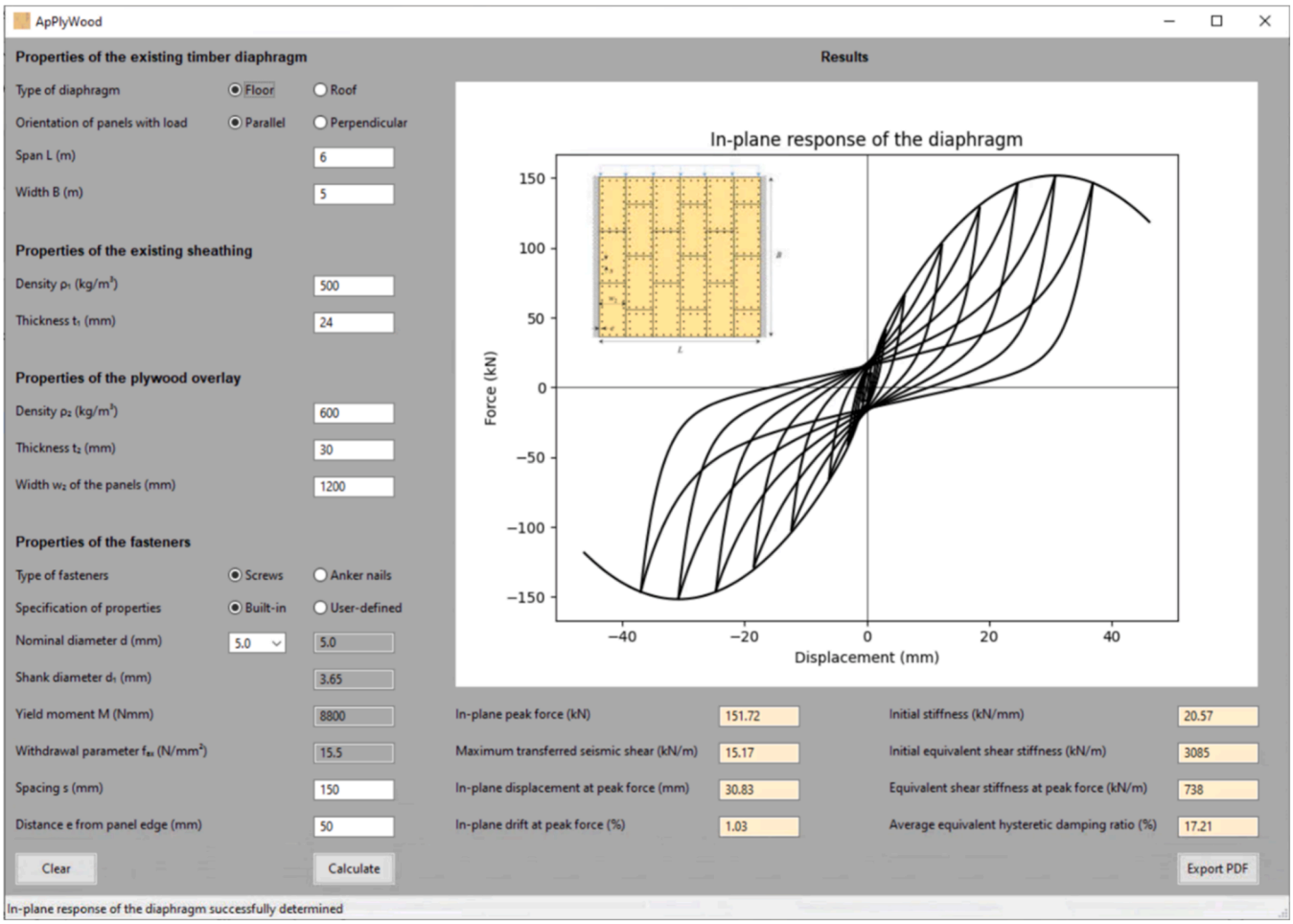

Fig. 9. Second calculation example executed with *ApPlyWood*.

be downloaded at the following link: https://doi.org/10.4121/b2588d43–7365-422f-8a73–8071e16c5e1c. Both the original script *SimPlyWood.f90* and the ready-to-use library *SimPlyWood.dll* to be provided in DIANA FEA are included. Besides, a spreadsheet *SimPlyWood_input* is also present, to directly convert the in-plane response of the retrofitted diaphragm estimated with *ApPlyWood* calculation tool (Section 2.2), to the user-supplied variables to be input in DIANA FEA. In the worksheet, the following parameters from *ApPlyWood* calculation tool have to be inserted: displacement at peak force $d_{max,floor}$, peak force $F_{max,floor}$, initial stiffness $K_{0,floor}$, span and width of the diaphragm, fastener type. Next, the number of macro-elements along the span (n) and the width (m) have to be provided. Assuming for convenience a unitary cross Section (1 mm^2) of the nonlinear diagonal trusses, the spreadsheet provides the related user input parameters for DIANA FEA by considering the following geometrical relationships (Fig. 5):

$$\varepsilon_{\max} = \frac{4d_{\max,floor}\cos\alpha}{l_d n} \tag{14}$$

$$\sigma_{\max} = \frac{F_{\max,floor}}{4m\cos\alpha} \tag{15}$$

$$K_0 = \frac{K_{0,floor} l_d n}{16 d_{\max,floor} m\cos\alpha} \tag{16}$$

The parameters resulting from Eqs. 14–16 allow to model in DIANA FEA the in-plane response of a diaphragm calculated with *ApPlyWood* tool, under a distributed (seismic) in-plane load: a full example of such procedure is provided in Section 4. Furthermore, if desired, it is also possible to adopt a more simplified modelling approach, considering a linear elastic (equivalent) response of the retrofitted diaphragms. In this case, Eq. 16 can also be employed to convert their global initial (or secant) elastic stiffness into the axial stiffness to be assigned to the diagonal truss elements. Because these elements would then be simply linear elastic with this approach, it is sufficient to only specify such determined axial stiffness in DIANA FEA, without needing to provide the user-supplied subroutine library.

3. Design tools

3.1. Nomograms

The nomograms derived according to Section 2.2 are reported in Fig. 6, from which the transferred seismic shear or the equivalent shear stiffness can be graphically determined as a function of the spacing of the screws. The corresponding nomograms for the coefficients k_t, $k_{\rho,v}$, and $k_{\rho,G}$ are shown in Fig. 7. The reported diagrams are now employed to present two calculation examples, in which the implemented tool *ApPlyWood* is used as well.

3.2. ApPlyWood calculation tool and examples

3.2.1. Example 1

As first calculation example, a floor retrofitted with plywood panels of width 600 mm, subjected to an in-plane distributed load perpendicular to their long side, is considered. The reference configuration assumed in Section 2.2 is considered, thus the coefficients reported in Fig. 7 are all unitary. Screws of diameter 4.5 mm at 100 mm spacing are

Table 1
Tested timber diaphragms from literature adopted in the comparison and main input parameters for the calculation tool; the variations compared to the original tested configurations are reported in the footnotes. For the samples from [13], the terms *PARA* and *PERP* refer to the loading direction parallel or perpendicular to the joists, while the panels' long side was oriented in the opposite direction.

Sample	OSB0-R [7]	OSB90-R [7]	MAE-2B [11]	DF-par1s [15]	DF-per4s [15]	B_Plyw [14]	R1 [12]	1b-PARA [13]	1b-PERP [13]
Diaphragm type	Roof	Roof	Floor	Roof	Roof	Floor	Floor	Floor	Floor
Panels' orientation with respect to load	Parallel	Perpendicular	Perpendicular	Perpendicular	Parallel	Perpendicular	Parallel	Perpendicular	Parallel
L (m)	3.0	6.0[b]	7.3	4.8[e]	2.4	9.6	9.6 [h]	10.4	5.5
B (m)	1.5[a]	1.5[a]	3.7	1.9 [f]	1.9 [f]	4.7	3.0	5.5	10.4
ρ_1 (kg/m^3)	473	473	450	440	440	500	450	450	450
t_1 (mm)	23	23	19	18	18	22	25	18	18
ρ_2 (kg/m^3)	555	555	500	470	470	550	500	500	500
t_2 (mm)	25	25	9.5	18	18	9	19	15	15
w_2 (mm)	1000	1000	1220	670	800	1200	1200	1200	1200
Fastener	Nails	Nails	Nails	Screws	Screws	Screws	Screws	Nails	Nails
d (mm)	3.1	3.1	3.1	4.5	5.0	3.5	4.5	3.1	3.1
d_1 (mm)	3.1	3.1	3.1	3.2	3.0	2.45	3.2	3.1	3.1
M_y (Nmm)	5700	5700	5700	5800	5400	2700	5800	5700	5700
f_{ax} (MPa)	7.0	7.0	7.0	17.0	11.7	17.9	17.0	7.0	7.0
s (mm)	150	214[c]	125[d]	100	100	110 [g]	75[i]	100	100
e (mm)	20	20	10	50	50	10	10	20	20

[a]The actual width of the sample was 3.0 m; the value was halved since the calculation tool provides the full strength of the floor considering both reactions at supports, whereas in the test only one supported floor portion was investigated.
[b]The actual span of the sample was 3.0 m; the value was doubled for this specific case to account for a different static scheme, since the calculation tool provides the load-displacement capacity under a distributed load, while in the test this floor portion was subjected to a concentrated load.
[c]The sample was retrofitted placing two nails at each beam intersection. With 7 beams, 14 nails were present, equivalent to a spacing of 3000/14 = 214 mm.
[d]The actual spacing around the panels' perimeter only was 150 mm; the reported value also accounts for the presence of field nailing within each panel.
[e]The actual span of the sample was 2.4 m; the value was doubled for this specific case to account for a different static scheme, since the calculation tool provides the load-displacement capacity under a distributed load, while in the test this floor portion was subjected to a concentrated load.
[f]The actual width of the sample was 3.8 m; the value was halved since the calculation tool provides the full strength of the floor considering both reactions at supports, whereas in the test only one supported floor portion was investigated.
[g]The actual spacing around the perimeter only was 150 mm; the reported value also accounts for the presence of field nailing within each panel.
[h]The actual span of the sample was 4.0 m; the value was set at 9.6 m for this specific case to account for the fact that the particular configuration of the floor and experimental setup allowed for eight sliding planes, in both panels and joists: to correct for this, the span was set as eight times the panels' width.
[i]The actual spacing around the perimeter only was 150 mm; the reported value also accounts for the presence of additional screws along the joists.

used for the retrofitting. From the top left nomogram of Fig. 6, under the assumed configuration, $v \approx 19$ kN/m and $G_d \approx 700$ kN/m are derived for the adopted fasteners and spacing.

Considering a floor having dimensions $B \times L = 3.8 \times 4.8$ m under distributed load q, these values from the nomogram would correspond to a transferred force of $v \cdot B = q \cdot L/2 = 19 \cdot 3.8 = 72.2$ kN, and thus to a global strength $q \cdot L$ of 144.4 kN; the related displacement under the assumption of distributed in-plane load would be $q \cdot L^2/(8 \cdot G_d \cdot B) = 144.4 \cdot 4.8/(8 \cdot 700 \cdot 3.8) = 32.57$ mm. This can be further confirmed by means of the implemented calculation tool, providing the same properties as input: very close outcomes are obtained (Fig. 8).

3.2.2. Example 2

In a second example, a $B \times L = 5 \times 6$ m floor strengthened with 1200×2400 mm panels is considered, subjected to an in-plane distributed load parallel to their long side. The following parameters are assumed: sheathing thickness $t_1 = 24$ mm and density $\rho_1 = 500$ kg/m^3; plywood thickness $t_2 = 30$ mm and density $\rho_2 = 600$ kg/m^3; screws of diameter 5.0 mm at 150 mm spacing.

In this loading configuration, the bottom right nomogram of Fig. 6 is used, from which values of $v \approx 13$ kN/m and $G_d \approx 570$ kN/m are derived for the adopted fastener and spacing. Now, the adjustments factors are determined from Fig. 7 to account for the actual properties of the diaphragm: with $t_1 = 24$ mm and $t_2 = 30$ mm, $k_t = 1.09$; with $\rho_1 = 500$ kg/m^3 and $\rho_2 = 600$ kg/m^3, $k_{\rho,v} = 1.10$ and $k_{\rho,G} = 1.09$. Inserting these parameters in Eqs. 4 and 5 provides an estimation of $v' \approx 15.5$ kN/m and $G'_d \approx 745$ kN/m.

The obtained values are very close to the actual parameters resulting from the calculation tool (Fig. 9). Therefore, the proposed nomograms enable an expeditious design of the retrofitting, and practitioners can benefit from the additional advantage of graphically visualizing how the different geometrical and material properties contribute to the final in-plane response of the diaphragms.

3.2.3. Comparison with previous research studies

The previous calculation examples showed that the developed tools can estimate well the in-plane response of diaphragms strengthened with plywood panels. For additional validation, *ApPlyWood* calculation tool is now used to determine the in-plane response of similarly retrofitted diaphragms tested in reference research studies from literature [7, 11,12–15]. In some cases, the static scheme or position of the fasteners did not correspond to the configuration at the basis of the calculation tool, i.e. a diaphragm retrofitted with plywood panels fastened along their perimeter under distributed load. However, these differences could be taken into account by means of geometrical and equilibrium-related considerations. Table 1 reports the reference samples examined in this comparison, along with the input values for the calculation tool and the variations with respect to the originally tested diaphragms.

Fig. 10 shows the outcomes of this analysis by comparing the backbones determined from *ApPlyWood* calculation tool to those experimentally recorded and (when available) retrieved with numerical analyses performed within the same studies from literature. For the floors where the panels were fastened to the existing planks with screws (Fig. 10d–g), the nomograms reported in Section 3.1 can also be used to estimate the strength and, through the equivalent shear stiffness at peak load G_d, the corresponding in-plane displacement. Thus, the values retrieved from the nomograms are included in the graphs of Fig. 10d–g, with an error range of 1–9 % in terms of peak strength, and of 3–11 % for the corresponding displacement, in comparison to the experiments.

In general, the calculation tool provides an accurate estimate of the in-plane response, well representing the behaviour from the initial elastic loading phase until peak strength independently of the fastener type (nails or screws). Some differences might arise in the post-peak phase, since the analytical curve implemented in the calculation tool

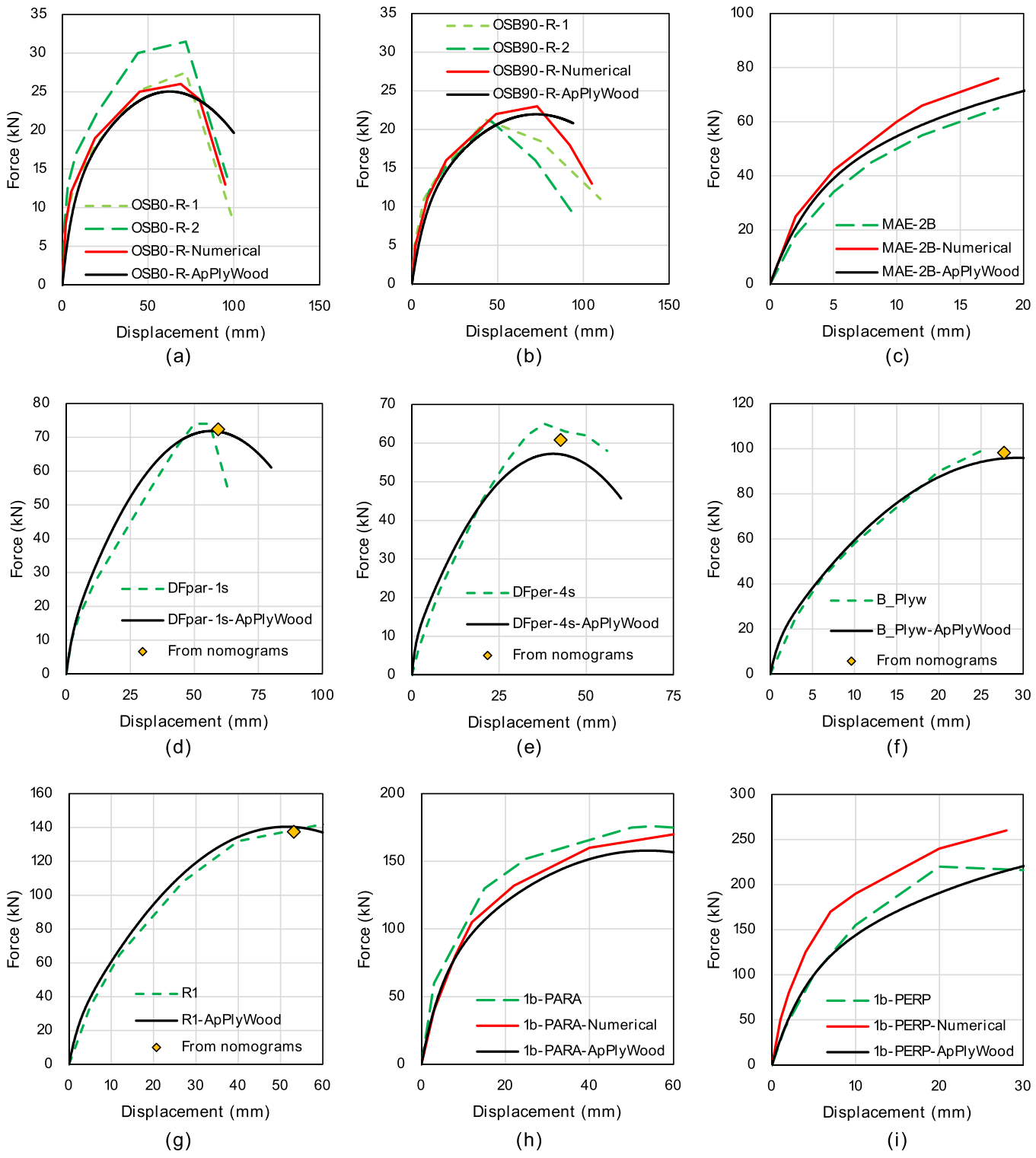

Fig. 10. Comparison between the outcomes from *ApPlyWood* calculation tool and the relevant selected studies from literature presented in Table 1: (a, b) experimental results and numerical analyses from Gubana and Melotto [7,52]; (c) experimental results from Peralta et al. [11,30] and numerical analyses from Masroor et al. [53]; (d, e) experimental results from Mirra et al. [15]; (f) experimental results from Rizzi et al. [14]; (g) experimental results from Brignola et al. [12]; (h, i) experimental results from Wilson et al. [13] and numerical analyses from Rizzi et al. [14]. For the diaphragms strengthened with plywood panels screwed to the existing sheathing (d, e, f, g), also the values from the nomograms of Section 3.1 are reported.

accounts for a progressive plasticisation of the fasteners assuming the occurrence of two plastic hinges at the plywood-planks interface (Section 2.1), while in some of the experiments slightly more sudden drops in strength can be observed, related to local brittle failures in the timber members.

An interesting outcome is also that the calculation tool can accurately reproduce the in-plane response of timber floors where an optimized plywood overlay layout was applied [14], maximising panels' interlocking (Fig. 10f) and leading to a more isotropic response; this type of retrofitting can be effectively schematised by considering a panels'

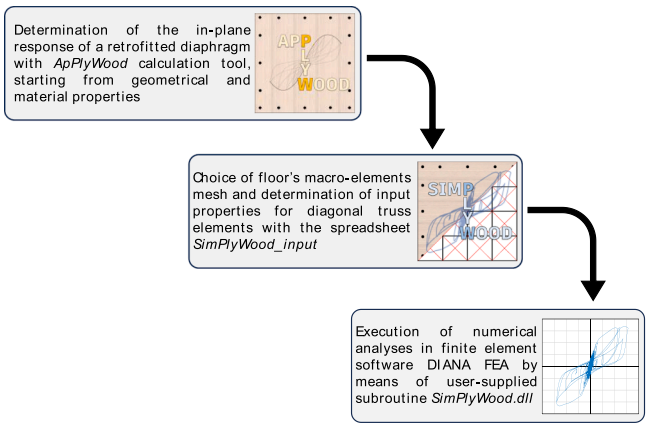

Fig. 11. Workflow for numerical modelling of plywood-retrofitted timber diaphragms starting from the in-plane response determined with the design tools.

orientation perpendicular to the seismic loads, where this interlocking effect is taken into account. It is also interesting to notice that, although the tool has been developed considering plywood panels as strengthening elements, good agreement with the experiments is also obtained for the diaphragms retrofitted with OSB panels (Table 1 and Fig. 10a–b). Based on these outcomes, further research work is envisaged to extend the calculation tool for taking into account other timber-based retrofitting methods besides the plywood overlay, such as the use of OSB or CLT panels, which are also commonly adopted in the seismic strengthening of wooden floors in existing masonry buildings (Section 1.1).

4. Modelling tools

4.1. General

The developed modelling tools allow to transform the in-plane response of a retrofitted diaphragm estimated with *ApPlyWood* calculation tool into a set of input values for the user-supplied subroutine in DIANA FEA software. An overview of this workflow is shown in Fig. 11: the user can first adopt *ApPlyWood* calculation tool to derive the main output parameters defining the in-plane response of the diaphragm (displacement at peak force, strength, initial stiffness and fastener type, see Section 2.3), starting from geometrical and material properties of floor and plywood, and mechanical characteristics of fasteners (Section 4.2). Next, by means of the spreadsheet *SimPlyWood_input*, these output parameters can be converted into the input values for the user supplied subroutine, by specifying the geometry of the macro-elements' mesh to be modelled in DIANA FEA. Finally, such calculated values can be specified when defining the material properties of the diagonal truss elements in DIANA FEA, where nonlinear numerical analyses can be conducted (Section 4.3).

4.2. Evaluation of in-plane response of a reference retrofitted diaphragm with ApPlyWood calculation tool

As reference example for the utilization of the implemented modelling tools, a floor $B \times L = 4.0 \times 6.0$ m retrofitted with plywood panels of width 600 mm, subjected to an in-plane distributed load perpendicular to their long side, is considered. For geometrical and material properties, the reference configuration assumed in Section 2.2 is considered, and both the use of 4.5 mm diameter screws (Fig. 12a) and of 4.0 mm diameter Anker nails (Fig. 12b), is examined.

4.3. Creation of the numerical model in DIANA FEA adopting SimPlyWood user-supplied subroutine and associated spreadsheet

The numerical model constructed in DIANA FEA 10.4 consisted of six macro-elements along the span and four along the width (Fig. 13), composed of unitary-cross-section rigid and diagonal truss elements (*L2TRU* [41]), the latter incorporating the governing in-plane response of the diaphragm as estimated from *ApPlyWood* calculation tool (Section 2.3). The macro-elements were overlapped to linear elastic plate elements (*Q20SF* [41]), having a thickness of 36 mm (sum of sheathing and plywood thicknesses), a negligible in-plane stiffness ($G_{xy} = 0.1$ MPa), and a mass density of 4910 kg/m^3, corresponding to a seismic weight of 1.77 kN/m^2, which incorporated the self-weight of the floor elements, an additional dead load of 1.00 kN/m^2, and 30% of a 2.00 kN/m^2 live load, following the seismic combination of EN 1998–1:2004 [54].

The spreadsheet *SimPlyWood_input* was first employed: by inserting the relevant values from *ApPlyWood* calculation tool, the input parameters for DIANA FEA were determined and adopted for the user-supplied material of the diagonal truss elements, considering either the retrofitting with screws (Fig. 13a) or nails (Fig. 13b), described in Section 4.1. The floor was hinged on the short sides and subjected to an in-plane earthquake signal perpendicular to the long side (Fig. 13c), to assess the accuracy of the user-supplied subroutine in representing the diaphragm's in-plane seismic response. Nonlinear dynamic (time-history) analyses were performed, adopting time steps of 0.005 s, and incorporating in the model the user-supplied subroutine library *SimPlyWood.dll*.

The obtained in-plane seismic response for the diaphragm is reported in Fig. 14a for the configuration retrofitted using screws, and in Fig. 14b for that featuring nails; the graphs show the seismic shear of the diaphragm against its midspan in-plane deflection. As can be noticed, the adopted modelling strategy and associated subroutine allow to accurately reproduce the full nonlinear behaviour of the strengthened diaphragm, including pinching phenomena. The obtained response is also in line with that estimated from *ApPlyWood* calculation tool, previously shown in Fig. 12. Therefore, the presented approach can support the effective (preliminary) design and advanced numerical modelling of timber diaphragms retrofitted with plywood panels.

5. Summary and conclusions

This article has presented a set of tools that can support the design and advanced numerical modelling of plywood-based seismic retrofitting interventions on existing timber diaphragms. Firstly, the derivation of nomograms for an expeditious design of this strengthening solution, has been presented. The nomograms, developed for screws on the basis of previously formulated analytical models, refer to two different commonly employed widths of the plywood panels (600 mm or 1200 mm), as well as two loading configurations (parallel or perpendicular to the panels' long side). The graphs allow to determine, as a function of the spacing of the fasteners, the corresponding transferred seismic shear v (in kN/m) and equivalent shear stiffness G_d at peak force (in kN/m). These values are based on a typical configuration featuring sheathing thickness $t_1 = 18$ mm and density $\rho_1 = 420$ kg/m^3; plywood thickness $t_2 = 18$ mm and density $\rho_2 = 500$ kg/m^3. In order to estimate v and G_d for different configurations, adjustment factors for these parameters have been determined as a function of other values of thickness and density, and have been presented in additional nomograms. In this way, practitioners can also graphically visualize how the different geometrical and material properties contribute to the in-plane response of a plywood-retrofitted diaphragm.

Second, a calculation tool (*ApPlyWood*) was implemented, allowing the users to obtain an estimate of strength, stiffness, and dissipative properties of diaphragms retrofitted with plywood panels, as well as to visualize their nonlinear, cyclic response. The use of the derived nomograms and calculation tool has been exemplified and validated against reference experimental tests from literature.

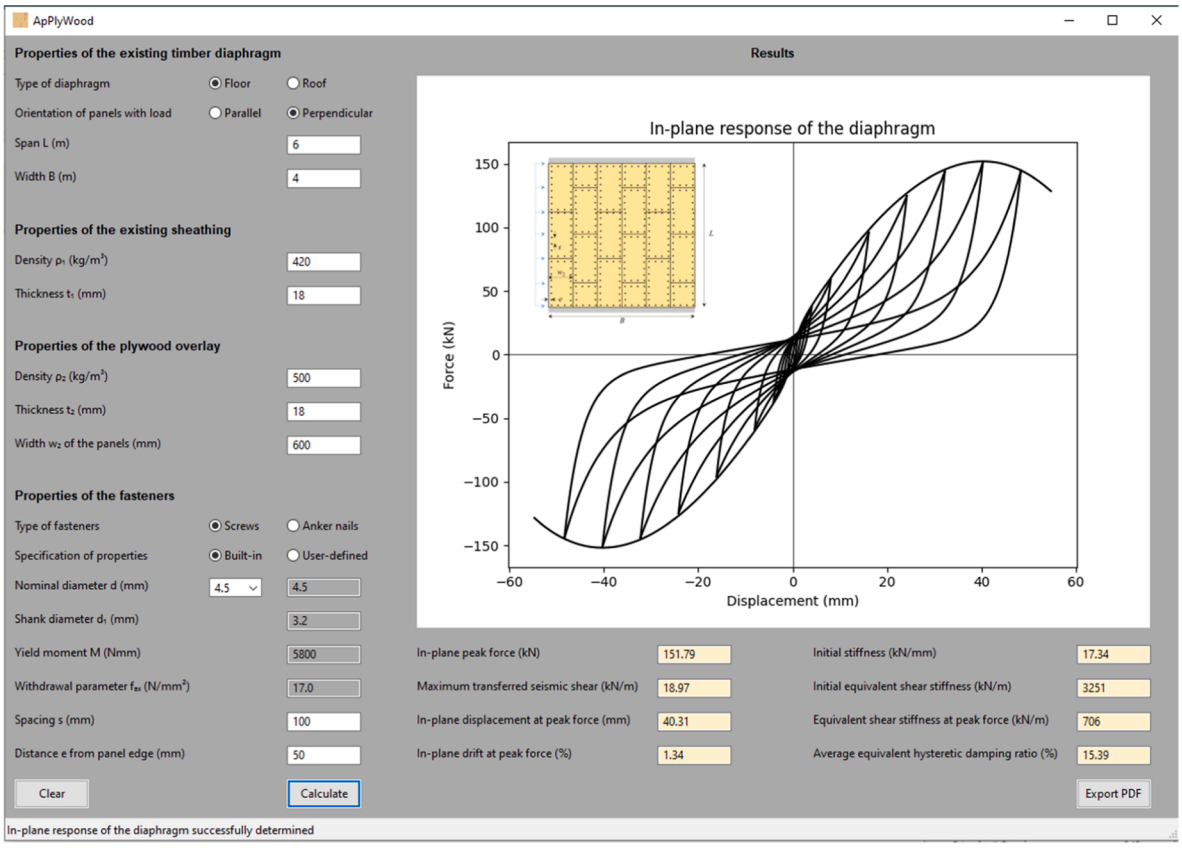

(a)

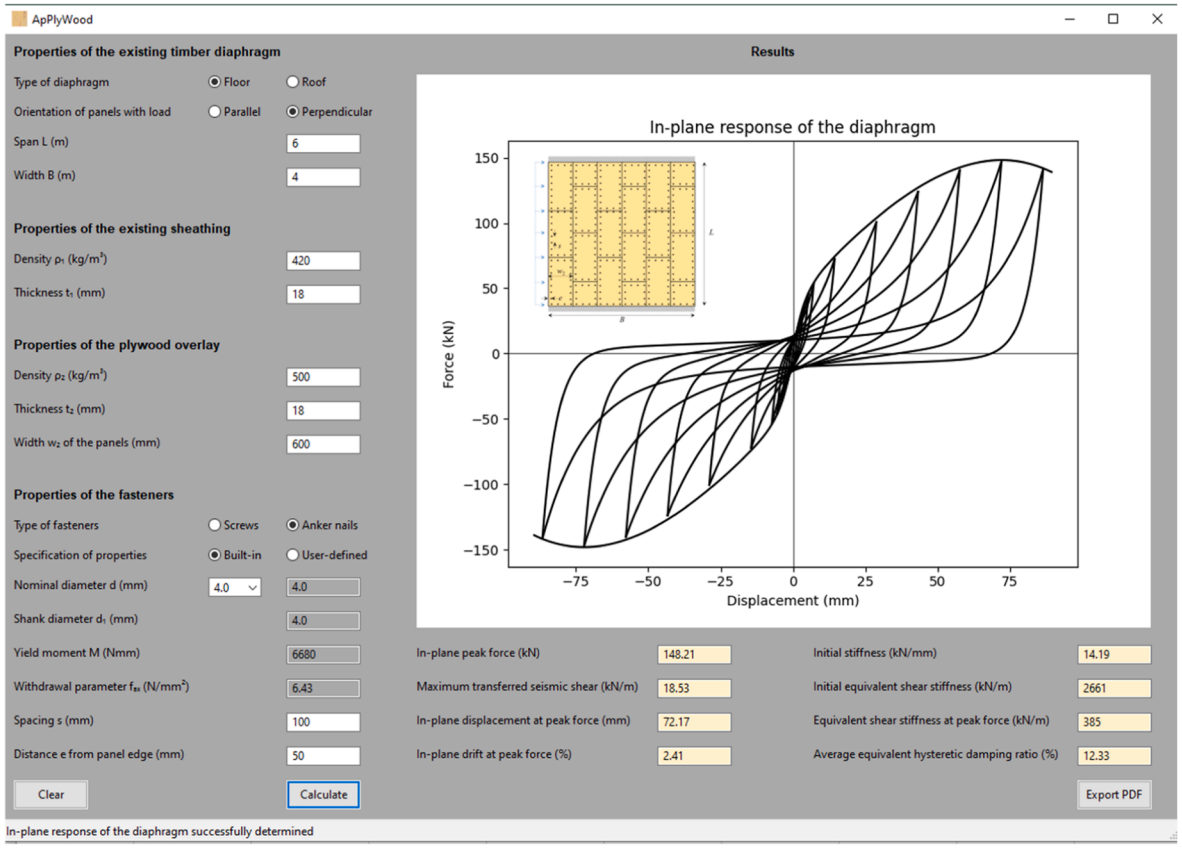

(b)

Fig. 12. Examples of calculated in-plane response from *ApPlyWood* to be used as input for the numerical model: floor retrofitted with plywood panels fastened with screws (a) or nails (b) to the existing sheathing.

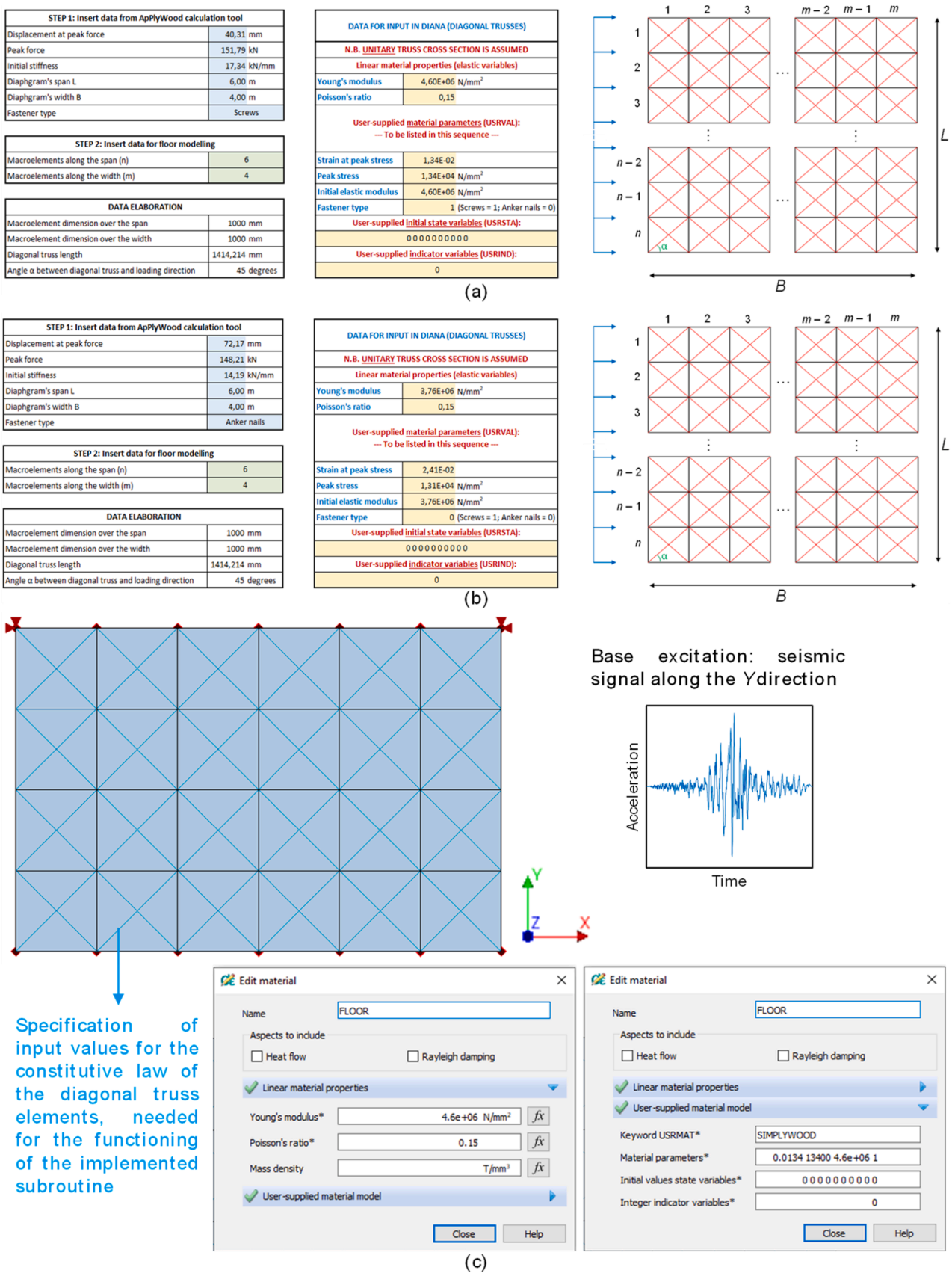

Fig. 13. Example of macro-element numerical model in DIANA FEA of the retrofitted timber diaphragm examined in Fig. 12: determination of input properties with *SimPlyWood_input* spreadsheet when screws (a) or nails (b) are used for the retrofitting; (c) view of model, adopted seismic signal for time-history analyses, and specification of input values for diagonal truss elements in the configuration with screws.

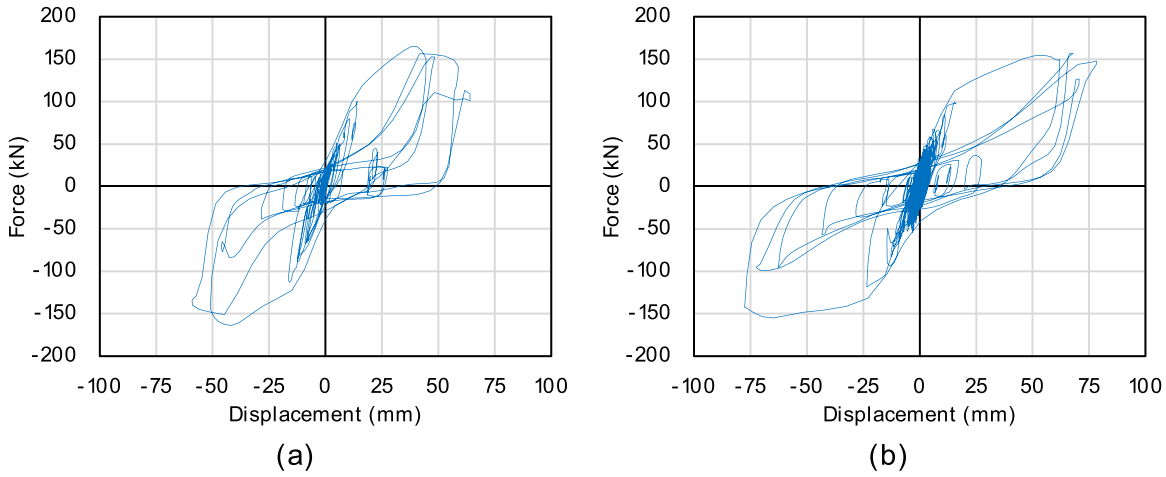

Fig. 14. Results of the numerical time-history analyses: force-displacement response of the diaphragm retrofitted using screws (a) and nails (b).

Third, a user-supplied subroutine (*SimPlyWood*) for DIANA FEA software was implemented, enabling the numerical simulation of the in-plane seismic response of the retrofitted diaphragms by means of a macro-element modelling strategy. Through a dedicated spreadsheet, the output values from *ApPlyWood* calculation tool can be transformed into the input parameters, to be provided in DIANA FEA, for the constitutive laws of the macro-elements simulating the in-plane response of the floors. The results show that the adopted modelling strategy can be utilized to effectively simulate the nonlinear seismic behaviour of the diaphragms, as proved by the presented example, where a 4 × 6 m diaphragm retrofitted with screwed or nailed plywood panels was subjected to time-history analyses.

In conclusion, the developed tools can be used to both obtain preliminary indications and calibrate the retrofitting interventions according to the specific needs of a building, supporting an integrated approach for design and modelling of the diaphragms, and relying on the adaptability and versatility of the plywood-based strengthening method. The presented collection of tools can be downloaded at the following link: https://doi.org/10.4121/8a09d423–2acc-4c7f-86af-90b5adca4660.

The outcomes of this work can contribute to the research framework supporting the use of timber-based techniques for the seismic upgrading and architectural conservation of existing and historical structures.

CRediT authorship contribution statement

Michele Mirra: Conceptualization, Data curation, Formal analysis, Investigation, Methodology, Software, Validation, Visualization, Writing – original draft, Writing – review & editing.

Declaration of Competing Interest

The authors declare that they have no known competing financial interests or personal relationships that could have appeared to influence the work reported in this paper.

References

[1] Piazza M., Baldessari C., Tomasi R. The Role of In-Plane Floor Stiffness in the Seismic Behaviour of Traditional Buildings. 14th World Conference on Earthquake Engineering, Beijing, China, 2008.
[2] Modena C., Valluzzi M.R., Garbin E., da Porto F. A strengthening technique for timber floors using traditional materials. Proceedings of the Fourth International Conference on Structural Analysis of Historical Constructions SAHC 04, Padua, Italy, 2004.
[3] Valluzzi M.R., Garbin E., Dalla Benetta M., Modena C. In-Plane Strengthening of Timber Floors For The Seismic Improvement Of Masonry Buildings. 11th World Conference on Timber Engineering, Riva del Garda, Italy, 2010.
[4] Gattesco N., Macorini L. High reversibility technique for in-plane stiffening of wooden floors. Proceedings of the VI International Conference on Structural Analysis of Historic Construction, Bath, United Kingdom, 2008.
[5] Corradi M, Speranzini E, Borri A, Vignoli A. In-plane shear reinforcement of wood beam floors with FRP. Compos Part B 2006;37:310–9.
[6] Branco JM, Kekeliak M, Lourenço PB. In-plane stiffness of timber floors strengthened with CLT. Eur J Wood Wood Prod 2015;73:313–23.
[7] Gubana A, Melotto M. Experimental tests on wood-based in-plane strengthening solutions for the seismic retrofit of traditional timber floors. Constr Build Mater 2018;191:290–9.
[8] Rizzi E., Capovilla M., Piazza M., Giongo I. In-plane behaviour of timber diaphragms retrofitted with CLT panels. Chapter in book: R. Aguilar et al. (Eds.): Structural Analysis of Historical Constructions, RILEM Bookseries 18:1613–1622, 2019.
[9] Longarini N, Crespi P, Zucca M. The influence of the geometrical features on the seismic response of historical churches reinforced by different cross lam roof-solutions. Bull Earthq Eng 2022;20:6813–52.
[10] Miglietta M, Damiani N, Guerrini G, Graziotti F. Full-scale shake-table tests on two unreinforced masonry cavity-wall buildings: effect of an innovative timber retrofit. Bull Earthq Eng 2021;19:2561–96.
[11] Peralta DF, Bracci MJ, Hueste MBD. Seismic behavior of wood diaphragms in Pre-1950s unreinforced masonry buildings. J Struct Eng 2004;130:2040–50.
[12] Brignola A, Pampanin S, Podestà S. Experimental evaluation of the in-plane stiffness of timber diaphragms. Earthq Spectra 2012;28(4):1–23.
[13] Wilson A, Quenneville PJH, Ingham JM. In-plane orthotropic behavior of timber floor diaphragms in unreinforced masonry buildings. J Struct Eng 2014;140.
[14] Rizzi E, Giongo I, Ingham JM, Dizhur D. Testing and modeling in-plane behavior of retrofitted timber diaphragms. J Struct Eng 2020;146(2).
[15] Mirra M, Ravenshorst G, van de Kuilen JW. Experimental and analytical evaluation of the in-plane behaviour of as-built and strengthened traditional wooden floors. Eng Struct 2020;211:110432.
[16] Lin T-J, LaFave JM. Experimental structural behavior of wall-diaphragm connections for older masonry buildings. Constr Build Mater 2012;26:180–9.
[17] Moreira S., Oliveira D.V., Ramos L.F., Lourenço P.B., Fernandes R.P., Guerreiro J. Experimental study on the seismic behavior of masonry wall-to-floor connections. Proceedings of the 15th World Conference on Earthquake Engineering, Lisbon, Portugal, 2012.
[18] Moreira S., Ramos L.F., Oliveira D.V., Lourenço P.B., Mateus L. Developing a seismic retrofitting solution for wall-to-floor connections of URM with wood diaphragms. Proceedings of the 9th International Masonry Conference, Guimarães, Portugal, 2014.
[19] Dizhur D., Giaretton M., Ingham J.M. URM wall-to-diaphragm and timber joist connection testing. Proceedings of the 10th International Masonry Conference, Milan, Italy, 2018.
[20] Riccadonna D, Giongo I, Schiro G, Rizzi E, Parisi MA. Experimental shear testing of timber-masonry dry connections for the seismic retrofit of unreinforced masonry shear walls. Constr Build Mater 2019;211:52–72.
[21] Almeida JP, Beyer K, Brunner R, Wenk T. Characterization of mortar-timber and timber-timber cyclic friction in timber floor connections of masonry buildings. Mater Struct 2020;53:51.
[22] Mirra M, Ravenshorst G, de Vries P, Messali F. Experimental characterisation of as-built and retrofitted timber-masonry connections under monotonic, cyclic and dynamic loading. Constr Build Mater 2022;358:129446.
[23] Endo Y, Goda T. Pull-out test and numerical simulation of beam-to-wall connection: masonry in earthen mortar and hardwood timber. Eng Struct 2023;275 (A)):115206.
[24] Gubana A. State-of-the-art report on high reversible timber to timber strengthening interventions on wooden floors. Constr Build Mater 2015;97:25–33.

[25] Mirra M, Ravenshorst G, van de Kuilen JW. Comparing in-plane equivalent shear stiffness of timber diaphragms retrofitted with light and reversible wood-based techniques. Pr Period Struct Des Constr 2021;26(4).
[26] Ongaretto E, Pozza L, Savoia M. Wood-based solutions to improve quality and safety against seismic events in conservation of historical buildings. Int J Qual Res 2016;10(1):17–46.
[27] Scotta R, Trutalli D, Marchi L, Pozza L. Seismic performance of URM buildings with in-plane non-stiffened and stiffened timber floors. Eng Struct 2018;167:683–94.
[28] Parisi MA, Piazza M. Seismic strengthening and seismic improvement of timber structures. Constr Build Mater 2015;97:55–66.
[29] Agbabian M.S., Barnes S.B., Kariotis J.C. Diaphragm testing. In Methodology for mitigation of seismic hazards in existing unreinforced masonry buildings. El Segundo, CA, 1981: N. S. Foundation.
[30] Peralta D.F., Bracci J.M., Hueste M.B. Seismic performance of rehabilitated wood diaphragms. Ph.D. dissertation, Dept. of Civil Engineering, Texas A&M University, 2003.
[31] Giongo I, Wilson A, Dizhur DY, Derakhshan H, Tomasi R, Griffith MC, et al. Detailed seismic assessment and improvement procedure for vintage flexible timber diaphragms. Bull N Z Soc Earthq Eng 2014;47(2):97–118.
[32] Mirra M, Ravenshorst G, de Vries P, van de Kuilen JW. An analytical model describing the in-plane behaviour of timber diaphragms strengthened with plywood panels. Eng Struct 2021;235:112128.
[33] Mirra M., Sousamli M., Longo M., Ravenshorst G. Analytical and numerical modelling of the in-plane response of timber diaphragms retrofitted with plywood panels. 8th International Conference on Computational Methods in Structural Dynamics and Earthquake Engineering, COMPDYN 2021, Athens, Greece, 2021.
[34] Mirra M, Ravenshorst G. Optimizing seismic capacity of existing masonry buildings by retrofitting timber floors: wood-based solutions as dissipative alternative to rigid concrete diaphragms. Buildings 2021;11(12):604.
[35] Mirra M., Ravenshorst G. A seismic retrofitting design approach for activating dissipative behaviour of timber diaphragms in existing unreinforced masonry buildings. Current Perspectives and New Directions in Mechanics, Modelling and Design of Structural Systems - Proceedings of the 8th International Conference on Structural Engineering, Mechanics and Computation, Cape Town, South Africa, 2022.
[36] Mirra M, Gerardini A, Ravenshorst G. Application of timber-based techniques for seismic retrofit and architectural restoration of a wooden roof in a stone masonry church. Procedia Struct Integr 2022;44:1856–63.
[37] Mirra M, Gerardini A, Ghirardelli S, Ravenshorst G, van de Kuilen JW. Combining architectural conservation and seismic strengthening in the wood-based retrofitting of a monumental timber roof: the case study of St. Andrew's Church in Ceto, Brescia, Italy. Int J Arch Herit 2023.
[38] Giuriani E, Marini A. Wooden roof box structure for the anti-seismic strengthening of historic buildings. Int J Arch Herit 2008;2:226–46.
[39] Giuriani E, Marini A, Preti M. Thin folded shell for the renewal of existing wooden roofs. Int J Arch Herit 2015;10(6):797–816.
[40] Van Rossum G., Drake F.L. Python 3 Reference Manual. Scotts Valley, CA: CreateSpace, 2009.
[41] Ferreira D., Manie J. DIANA Finite Element Analysis. DIANA Documentation Release 10.4. DIANA FEA BV, Delft, The Netherlands.
[42] wxPython – The GUI toolkit for Pyton. https://wxpython.org.
[43] ISO 16670:2003. Timber structures — Joints made with mechanical fasteners — Quasi-static reversed-cyclic test method, International Organization for Standardization (ISO), Geneva, Switzerland.
[44] Dubas P., Gehri E., Steurer T. Einführung in die Norm SIA 164 (1981) – Holzbau. Publication No. 81–1, Baustatik und Stahlbau, ETH Zürich, Switzerland, 1981.
[45] EN 1995–1-1:2004+A2:2014. Eurocode 5: Design of timber structures - Part 1–1: General - Common rules and rules for buildings. Comité Européen de Normalisation (CEN), Brussels, Belgium.
[46] Johansen KW. Theory of timber connections. International Association of Bridge and Structural Engineering. Publication 1949;9:249–62.
[47] EN 409:2009. Timber structures - Test methods - Determination of the yield moment of dowel type fasteners. Comité Européen de Normalisation (CEN), Brussels, Belgium.
[48] Rotho Blaas Srl – Timber screws and deck fastening. Technical data catalogue, Cortaccia, Italy, 2023.
[49] Chopra AK. Dynamics of Structures. Theory and Applications to Earthquake Engineering. 3rd ed.,. Upper Saddle River: Prentice Hall; 2007.
[50] OpenSees ZeroLength Element, https://opensees.berkeley.edu/wiki/index.php/ZeroLength_Element.
[51] Ortega J.M. An Introduction to FORTRAN 90 for Scientific Computing. Saunders College Pub., Fort Worth, 1994.
[52] Gubana A, Melotto M. Cyclic numerical analyses on wood-based in-plane retrofit solutions for existing timber floors. Structures 2021;33:1764–74.
[53] Masroor A., Avanes C., Asghari M., Soroushian S., Smith R.J. Comprehensive finite element simulation of the flexible wood diaphragms. 16th World Conference on Earthquake Engineering, Santiago, Chile, 2017.
[54] EN 1998–1:2004. Eurocode 8: Design of structures for earthquake resistance – Part 1: General rules, seismic actions and rules for buildings. Comité Européen de Normalisation (CEN), Brussels, Belgium.